IMPROVEMENT OF THE SOUND TRANSMISSION LOSS OF PANELS BY MEANS OF ACOUSTICALLY TUNED RESONATORS

M.H.C. Hannink
Chair of Structural Dynamics and Acoustics
Department of Engineering Technology, University of Twente
P.O. Box 217, 7500 AE Enschede, The Netherlands
m.h.c.hannink@utwente.nl

Keywords: *sound, transmission, panels, resonators*

Abstract

When a panel is excited, either structurally or acoustically, sound is radiated from the panel. Previous research by the author has shown that tuned acoustic tube resonators can be used to reduce the radiated sound. A one-dimensional analytical model model was validated by experiments in an impedance tube and good agreement was found between model and measurements. In this paper, the model is extended to describe the sound transmitted through a panel with acoustic resonators. Two different configurations are examined: panels with tubes and perforated sandwich panels. To verify whether the one-dimensional analytical models give a good prediction of the sound transmission loss, panels of both configurations were tested. Sound transmission loss measurements were performed by means of the sound intensity method (ISO 15186-1). The measurements showed that the resonators indeed increased the transmission loss compared with the mass law, in the frequency range for which the resonators were tuned. However, the increase was not as large as predicted by the one-dimensional model. Resonators can be applied for various structural parts of an aircraft through which the transmission of sound has to be reduced. The research is performed as part of the EU project FACE (Friendly Aircraft Cabin Environment).

1 Introduction

Previous research has shown that the sound radiated by a vibrating panel can be reduced considerably by the application of tube resonators [1]. In this paper, the influence of tube resonators on sound transmission through a panel is examined. Two different configurations are considered: a thin plate with tubes attached to it (see Fig. 1) and a sandwich panel (see Fig. 2). The advantage of the last configuration is that it can be manufactured easily, for example, by perforating one of the skin panels of a common honeycomb (HC) sandwich panel (see Fig. 5). A one-dimensional analytical model is developed to predict the normal incident sound transmission of the two panel configurations. To verify whether the one-dimensional models give a good prediction of the sound transmission loss, measurements were performed on different resonator panels and compared with the analytical results.

The principle of sound reduction that is used is based on the local minimisation of the sound radiated by small partitions of the panel; a method that is also used in active acoustic control [7]. Ross applied a similar principle for passive noise control by means of so-called weak radiating cells [6]. With the tube resonators, maximum sound reduction is achieved if the volume velocities at the surface of the vibrating panel and

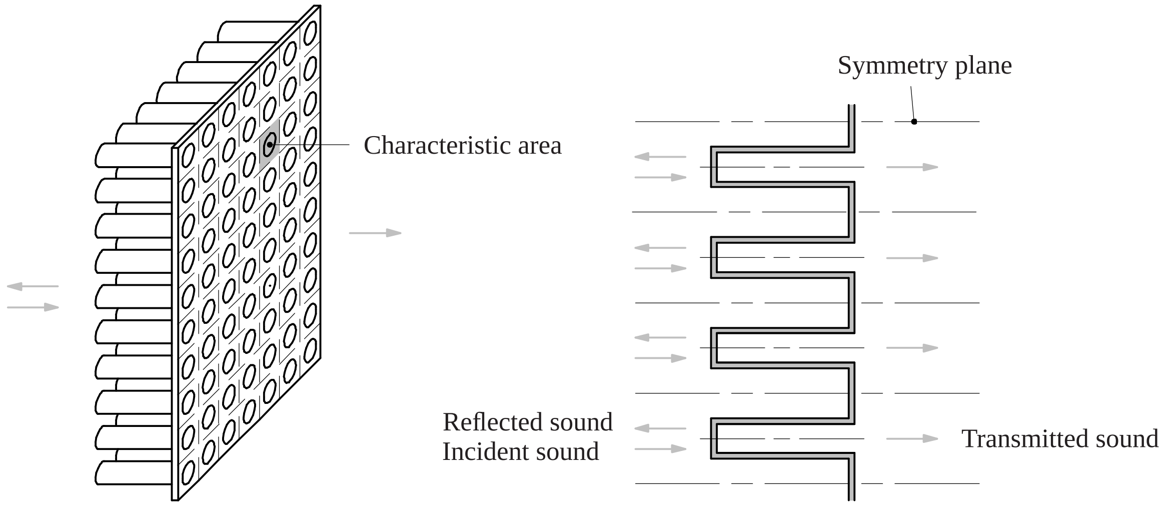

Fig. 1 Part of a panel with acoustic resonators divided into characteristic areas (left) and a schematic representation of the one-dimensional approach (right) - tube panel configuration.

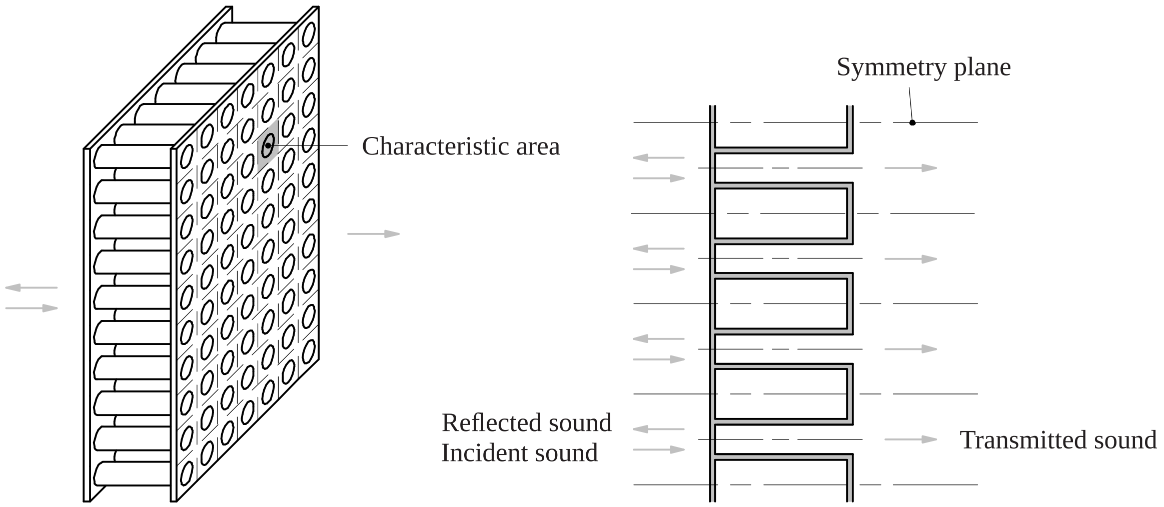

Fig. 2 Part of a panel with acoustic resonators divided into characteristic areas (left) and a schematic representation of the one-dimensional approach (right) - sandwich panel configuration.

those at the entrance of the resonators are equal in magnitude and opposite in phase. The frequency range in which the sound is reduced is determined by the length of the resonators. The centre frequency of this range is the frequency for which half of the acoustic wavelength corresponds with the length of the resonator. The shape of the spectrum is determined by the ratio of the cross-sectional areas of the resonators to the area of the panel.

2 One-dimensional analytical models

2.1 One-dimensional approach

In this section, an infinitely large, rigid panel with resonators is considered. Because of the repetitive pattern of the resonators in the panel, the panel can be divided into a number of so-called characteristic areas, each area containing one resonator (see Fig. 1). All characteristic areas are identical and assumed to be small compared with the acoustic wave length. Since the panel is considered to be rigid and infinitely large, the boundaries of these characteristic areas can be regarded as symmetry planes. Consequently, the velocity normal to the symmetry planes is assumed to be zero. The influence of the resonators on the sound that is transmitted in the normal direction through the panel can therefore be studied with a one-dimensional model of one characteristic area.

2.2 Transmission of sound through a rigid characteristic area

2.2.1 Models

Fig. 3 shows the model of a characteristic area of the tube panel. The model consists of four parts: the sound fields behind the panel, in front of the panel, inside the resonator, and around the resonator. Both the plate and the resonator are assumed to be rigid and vibrating harmonically with the same normal velocity amplitude u_s. The amplitude p_j of the harmonic pressure perturbation and the amplitude u_j of the harmonic velocity perturbation in axial direction ($j = 1,2,3,4$) for the different parts are given by the solution of the one-dimensional Helmholtz equation:

$$p_j(x) = A_j e^{\mathrm{i}kx} + B_j e^{-\mathrm{i}kx} \tag{1}$$

$$u_j(x) = -\frac{1}{\rho_0 c_0}\left(A_j e^{\mathrm{i}kx} - B_j e^{-\mathrm{i}kx}\right) \tag{2}$$

where i is the imaginary unit, x is the axial coordinate, ρ_0 is the density of air, c_0 is the speed of sound, and $k = \omega/c_0$ is the wave number, with ω the angular frequency. A_j and B_j are the complex amplitudes of the backward and forward travelling sound waves, respectively, determined by the boundary conditions of the four parts. The amplitude of the incident sound wave is denoted by B_4, the amplitude of the reflected sound wave by A_4, and the amplitude of the transmitted sound wave by B_2. Since the sound is radiated to the far-field, it is assumed that no reflection takes place and the amplitude A_2 equals zero. The radiated sound field is defined with reference to coordinate x_{II}. The other sound fields are defined with reference to coordinate x_{I} (see Fig. 3).

Boundary conditions at the right-hand side of the panel require that the particle velocity at the end of the resonator is equal to the structural velocity; the pressure perturbation is continuous at the entrance of the resonator; and conservation of mass holds for the control volume $\mathrm{CV_{II}}$ at the resonator entrance (see Fig. 3). At the left-hand side of the panel similar boundary conditions have to be satisfied. Furthermore, equilibrium of forces is required for the entire system. All together, these conditions can be written as:

$$\begin{aligned}
u_1|_{x_\mathrm{I}=0} &= u_s && (3)\\
p_1|_{x_\mathrm{I}=L} &= p_2|_{x_\mathrm{II}=0} && (4)\\
u_1|_{x_\mathrm{I}=L}\, S_r + u_s\,[S-S_r] &= u_2|_{x_\mathrm{II}=0}\, S && (5)\\
u_3|_{x_\mathrm{I}=L} &= u_s && (6)\\
p_3|_{x_\mathrm{I}=0} &= p_4|_{x_\mathrm{I}=0} && (7)\\
u_3|_{x_\mathrm{I}=0}\,[S-S_r] + u_s\, S_r &= u_4|_{x_\mathrm{I}=0}\, S && (8)\\
p_4|_{x_\mathrm{I}=0}\, S_r + p_3|_{x_\mathrm{I}=L}\,[S-S_r] + {}&\\
-p_1|_{x_\mathrm{I}=0}\, S_r - p_2|_{x_\mathrm{II}=0}\,[S-S_r] &= \bar{m}\mathrm{i}\omega u_s && (9)
\end{aligned}$$

where $\bar{m}$ is the structural mass of the characteristic area, S is the characteristic area, S_r is the cross-sectional area of the resonator, and L is the effective length of the resonator (see Section 2.2.2). By substitution of equations (3) to (9) into equations (1) and (2), the unknown pressure amplitudes A_1, B_1, B_2, A_3, B_3 and A_4 and the structural velocity amplitude u_s can be solved for a given incident pressure amplitude B_4.

For the sandwich panel configuration (see Fig. 4) a similar system of equations can be formulated. The boundary conditions described by equations (3) to (6) remain the same. The other boundary conditions change to:

$$\begin{aligned}
u_3|_{x_\mathrm{I}=0} &= u_s && (10)\\
u_4|_{x_\mathrm{I}=0} &= u_s && (11)
\end{aligned}$$

$$\begin{aligned}
p_4|_{x_\mathrm{I}=0}\, S - p_1|_{x_\mathrm{I}=0}\, S_r - p_3|_{x_\mathrm{I}=0}\,[S-S_r] + {}&\\
+ p_3|_{x_\mathrm{I}=L}\,[S-S_r] - p_2|_{x_\mathrm{II}=0}\,[S-S_r] &= \bar{m}\mathrm{i}\omega u_s
\end{aligned} \tag{12}$$

By substitution of equations (3) to (6) and (10) to (12) into equations (1) and (2), the unknown pressure amplitudes A_1, B_1, B_2, A_3, B_3 and A_4 and the structural velocity amplitude u_s can be solved again for a given incident pressure amplitude B_4.

The transmission coefficient τ is defined as the ratio between incident sound intensity and

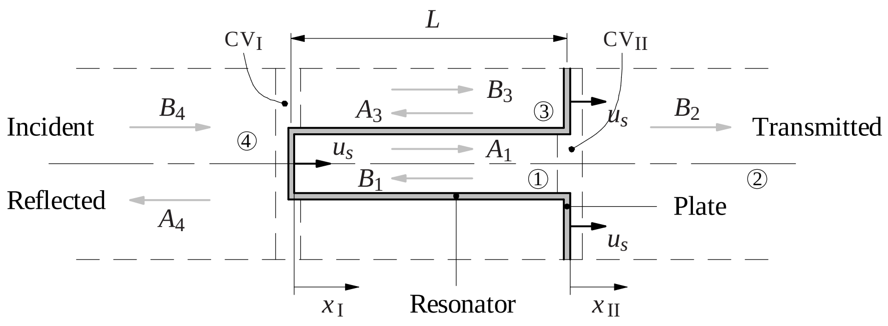

Fig. 3 Model of normal incidence transmission of sound through a rigid characteristic area - tube panel configuration.

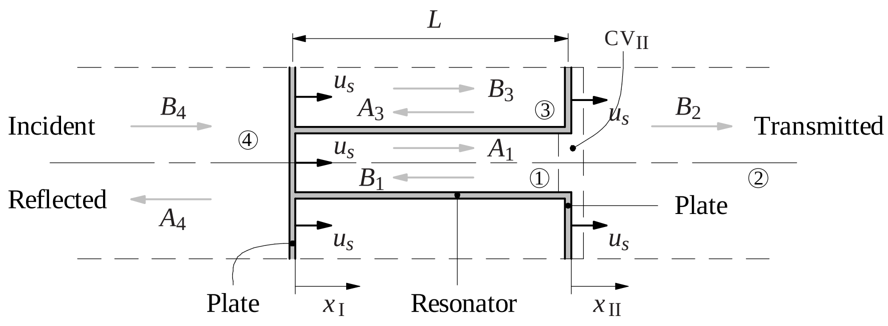

Fig. 4 Model of normal incidence transmission of sound through a rigid characteristic area - sandwich panel configuration.

transmitted sound intensity. For the presented models, this can be written as:

$$\tau = \left|\frac{B_2}{B_4}\right|^2 \tag{13}$$

The sound transmission loss is directly related to the transmission coefficient by:

$$TL = 10\log_{10}(1/\tau) \tag{14}$$

2.2.2 Results

With the models described above, the sound transmission loss is calculated for the three resonator configurations listed in Table 1: two tube panels and one perforated sandwich panel. $b = \sqrt{S}$ is the length of the sides of the square characteristic areas, and the porosity is defined by $\Omega = S_r/S$. For the two tube panels, the shear wave numbers [3] of the air inside and around the resonators are large. Therefore, viscothermal effects can be neglected. However, the shear wave numbers of the air inside the perforated HC structure are much smaller, because one resonator consists of several HC cells (see Fig. 5). Therefore, for this panel viscothermal effects have to be included. This is done by adjusting equations (1) and (2) for the air inside and around the resonators according to reference [3]. Due to inlet effects, the effective length of the resonator $L = L_{\text{phy}} + \delta$ is larger than the physical length of the resonator. For a perforated plate with a rectangular pattern, the end correction δ is given by [4]:

$$\delta = 0.79R\left[1 - 1.47\sqrt{\frac{\pi R^2}{b^2}} + 0.47\left(\frac{\pi R^2}{b^2}\right)^{3/2}\right] \tag{15}$$

Fig. 12, Fig. 13 and Fig. 14 show that a large increase in sound transmission loss is predicted over a broad frequency range compared with the mass law. The increase in transmission loss of the perforated HC sandwich panel is smaller than that of the tube panels. This is partly caused by viscothermal effects. Internal resonances in the cavities of the HC structure cause an extra peak and dip in the transmission loss curve at the frequency for which half of the wavelength corresponds with the length of the resonator.

3 Experiments

3.1 Experimental setup

Based on the theory described above, three resonator panels were designed on which sound transmission loss measurements were performed at the National Aerospace Laboratory NLR [2, 8]. The experimental setup is shown in Fig. 6. The test panel was mounted between two wooden frames with rubber stringers (see Fig. 7). Because of the large thickness of the HC sandwich panels, flanking noise had to be suppressed by covering the sides of these panels with lead (see Fig. 5). In the reverberation room, four speakers were placed near the corners and fed with white noise to generate sound in the frequency range of 500-5600 Hz. Another speaker, a so-called dodecahedron, was used to generate sound below 500 Hz. The sound in the reverberation room was measured by a microphone on a rotating boom, scanning the surface of a sphere. The sound is transmitted through the panel via a niche into a semi-anechoic receiving room. The semi-anechoic receiving room has a volume of about 205 m^3. To suppress the effect of reflections of the walls, sound absorbing material was installed around the niche. The 1 m $\times$ 1 m niche has a depth of about 0.87 m. The sound radiated by the panel was determined by measuring the sound intensity over the cross-section of the niche at a distance of about 0.74 m from the panel. The sound intensity was measured using the scanning method. For each panel, the sound transmission loss was determined by taking the average of a vertical scan and a horizontal scan (ISO 15186-1). Part of the measurements was performed by a scanning robot and part of the measurements was performed by hand. The scanning speed was approximately $75 \cdot 10^{-3}$ m/s.

3.2 Sound intensity method

As far as appropriate and possible, the sound transmission loss was measured according to ISO 15186-1. The sound transmission loss was determined by:

$$TL = (L_p)_{\text{avg}\ i} - (L_I)_{\text{avg}\ t} - 6\ \text{dB} \qquad (16)$$

where $(L_p)_{\text{avg}\ i}$ is the space-averaged sound pressure level in the reverberation room, measured with a microphone on a rotating boom, and $(L_I)_{\text{avg}\ t}$ is the sound intensity level normal to and averaged over the measuring surface in the receiving room, measured by a sound intensity probe with two microphones.

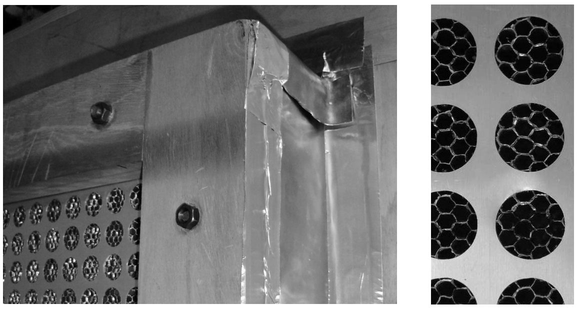

Fig. 5 Lead strips for flanking noise suppression of the HC sandwich panels (left) and detail of the perforated HC sandwich panel (right).

3.3 Test panels

Three resonator panels were tested. One panel consists of a thin perforated aluminium plate with plastic tube resonators. The other panel is a thin perforated aluminium plate with aluminium tube resonators (see Fig. 7). The third panel is an aluminium HC sandwich panel with one of the skin panels perforated (see Fig. 5). The resonators are tuned to achieve a large increase in sound transmission loss in the frequency range of 1000-2000 Hz. Table 1 shows the dimensions of the resonator configurations. The perforated HC sandwich panel is relatively stiff. To examine whether the sound transmission loss of a HC sandwich panel can be compared with the mass law, also an unperforated HC sandwich panel was tested. Both panels consist of a 0.109 m thick 2.3-1/4-10 (5052) Hexweb® aluminium HC core and two $5.6 \cdot 10^{-4}$ m thick aluminium skin panels. The mass of all panels and the plate thickness t of the tube panels are shown in Table 1.

	L_{phy} [m]	R [m]	b [m]	Ω [-]	t [m]	m [kg/m^2]
Panel with plastic tubes	0.114	$15.2 \cdot 10^{-3}$	$38.0 \cdot 10^{-3}$	0.50	$1.5 \cdot 10^{-3}$	5.65
Panel with aluminium tubes	0.109	$12.2 \cdot 10^{-3}$	$30.5 \cdot 10^{-3}$	0.50	$2.0 \cdot 10^{-3}$	9.74
Perforated HC sandwich panel	0.110	$12.5 \cdot 10^{-3}$	$31.5 \cdot 10^{-3}$	0.49	-	6.88
HC sandwich reference panel	-	-	-	-	-	8.13

Table 1 Dimensions and mass of the test panels.

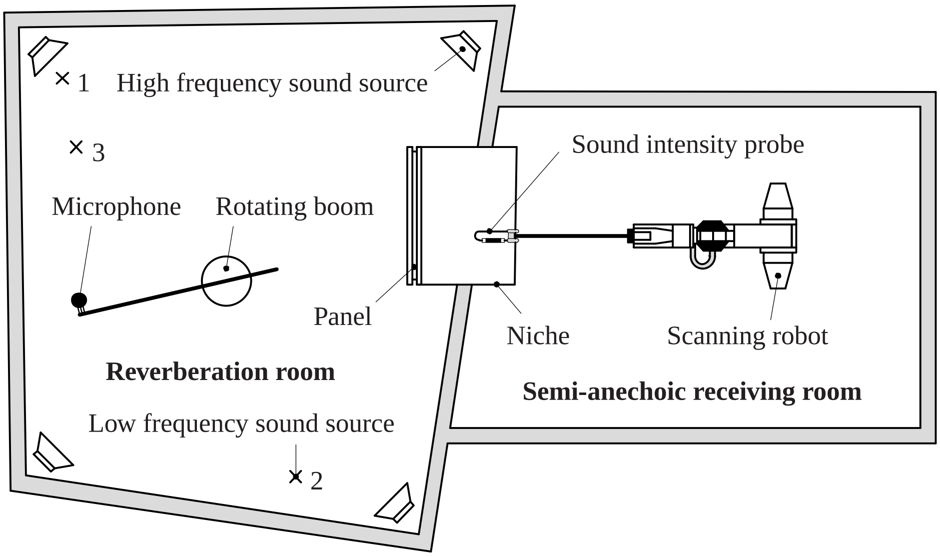

Fig. 6 Experimental setup for sound transmission loss measurements.

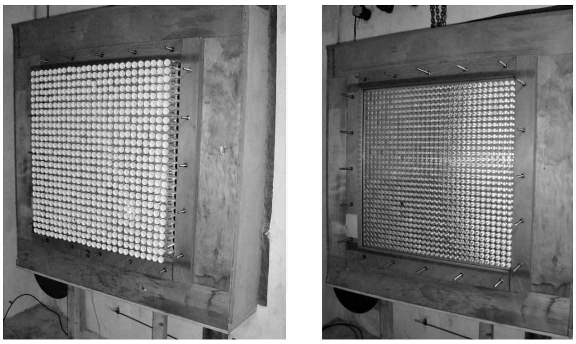

Fig. 7 Panel with plastic tubes (left) and panel with aluminium tubes (right).

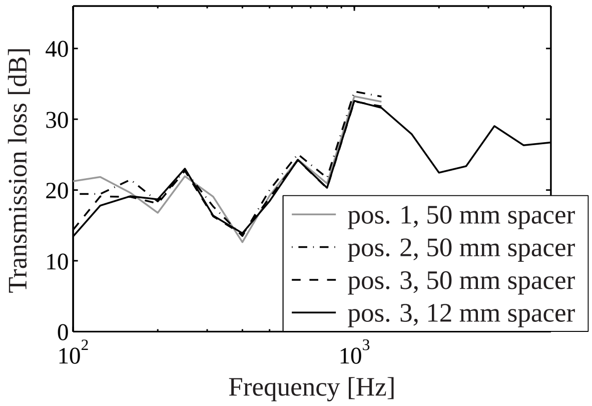

Fig. 8 Transmission loss of panel with plastic tubes for different speaker positions and spacer lengths.

3.4 Experimental results

The volume of the reverberation room is approximately 33 m^3, resulting in a diffuse sound field for frequencies of about 500 Hz and higher. To determine the measurement error due to insufficient diffusivity of the sound field below 500 Hz, sound transmission loss measurements were performed for three different positions of the low frequency sound source (see Fig. 6). Fig. 8 shows the measured transmission loss of the panel with plastic tubes for the different speaker positions. The results are presented in one-third octave bands (1/3OBs). Below the 160 Hz 1/3OB the accuracy is poor. From the 160 Hz 1/3OB to the 315 Hz 1/3OB the differences are within 2.8 dB. Above the 315 Hz 1/3 OB the differences are within 1.6 dB. Since the main focus for the tested panels is on the frequency range of 500 Hz and higher, this accuracy is considered to be sufficient. The other measurements presented in this section were performed by a sound intensity probe with a 12 mm microphone spacing and the dodecahedron located at position 3 (see Fig. 6).

Fig. 9 shows the measured transmission loss of the tube panels compared with the mass law. The dashed lines indicate the frequency range for which the resonators were tuned. To account for the effects of the boundedness of the panel and random incident sound, the normal incidence mass law is corrected according to ISO 15186-3:

$$TL_m = 10\log_{10}\left[1+\left(\frac{m\omega}{2\rho_0 c_0}\right)^2\right] - 10\log_{10}(2\sigma_d) \tag{17}$$

where m is the mass per unit area of the panel, and σ_d is the radiation efficiency of a flat square plate surrounded by an infinite rigid baffle, excited by a diffuse sound field. The radiation efficiency is approximated by [5]:

$$\sigma_d = \frac{1}{2}\left[0.2+\ln\left(\frac{\omega}{c_0}\sqrt{S_p}\right)\right] \tag{18}$$

where S_p is the area of the test panel.

In the 1000 Hz 1/3OB, the panel with plastic tubes shows an increase in transmission loss of 5.3 dB compared with the mass law. In the 250 Hz 1/3OB, an increase of 4.3 dB is obtained. For the other frequencies the transmission loss is smaller than obtained with the mass law. The panel with aluminium tubes shows increases of 7.1 dB in the 800 Hz 1/3OB and 3.9 dB in the 1600 Hz 1/3OB, compared with the mass law. The increase in transmission loss covers a much broader frequency range than that of the panel with plastic tubes. Only from the 2000 Hz 1/3OB, the transmission loss is again smaller than the mass law.

Fig. 10(a) shows the measured transmission loss of the HC sandwich reference panel compared with the mass law. From the 500 Hz 1/3OB, the differences between the measured transmission loss and the mass law are less than 3.0 dB. In the frequency range for which the resonators of the perforated HC sandwich panel were tuned, the differences are even smaller. Therefore, it can be concluded that, from the 500 Hz 1/3OB, the transmission loss of the perforated HC sandwich panel can be compared with the mass law. The first eigenfrequency of the HC sandwich reference panel is 395 Hz. Below this frequency the mass law is not valid. This is also seen in the measurements.

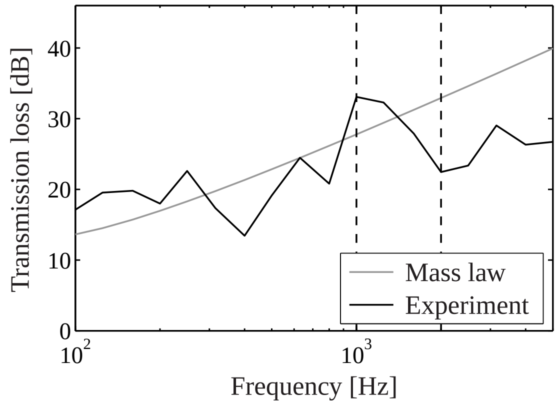

(a) Panel with plastic tubes

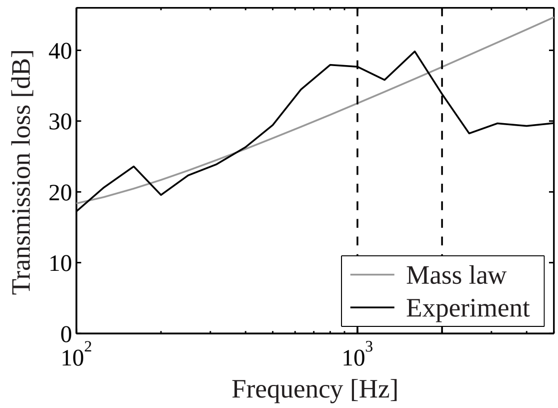

(b) Panel with aluminium tubes

Fig. 9 Transmission loss of tube panels compared with the mass law.

The measured transmission loss of the perforated HC sandwich panel is shown in Fig. 10(b). In the entire frequency range above the 500 Hz 1/3OB, the transmission loss of the perforated HC sandwich panel is larger than the mass law. The first eigenfrequency of the perforated HC sandwich panel is 375 Hz. Below this frequency, a comparison with the mass law is not valid. In the 1250 Hz 1/3OB, an increase in transmission loss of 7.2 dB is obtained compared with the mass law. In the 4000 Hz 1/3OB, an increase of 9.2 dB is observed. In the 630 Hz 1/3OB, an increase of 6.2 dB is obtained.

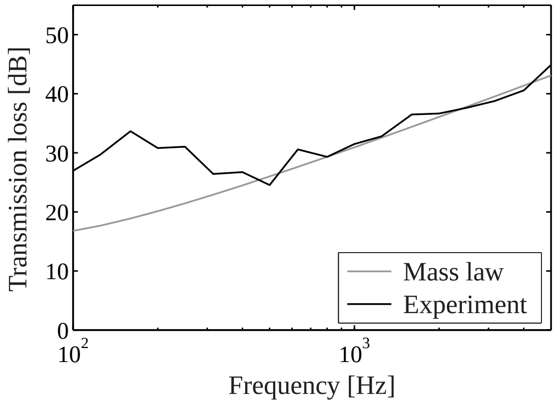

(a) HC sandwich reference panel

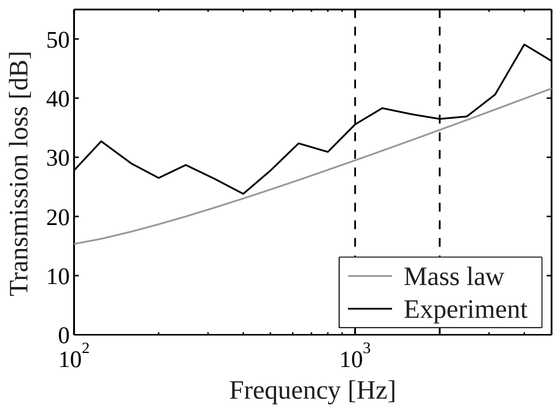

(b) Perforated HC sandwich panel

Fig. 10 Transmission loss of HC sandwich panels compared with the mass law.

3.5 Acoustic reciprocity

For the measurements presented above, the panels were mounted with the resonator openings at the receiving side. The principle of acoustic reciprocity states that the acoustic response remains the same when source and receiver are interchanged. To verify this, the panel with plastic tubes and the perforated HC sandwich panel were also tested with the resonator openings at the reverberation room side. Comparisons of both results are shown in Fig. 11. From the 500 Hz 1/3OB, the differences between the results of the panel with plastic tubes are less than 2.9 dB. For the perforated HC sandwich panel, the differences are less than 2.5 dB in this frequency range. It can be concluded that the orientation of the resonators does not have a large influence on the measured transmission loss.

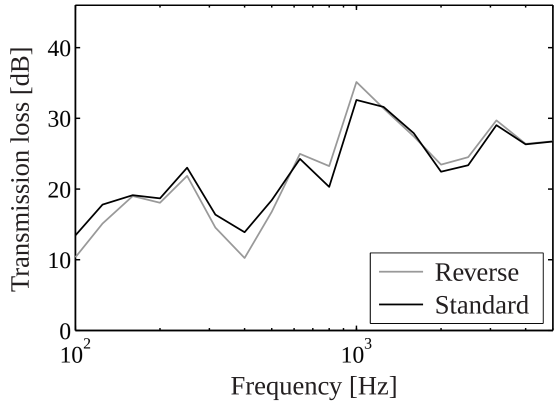

(a) Plastic tubes panel

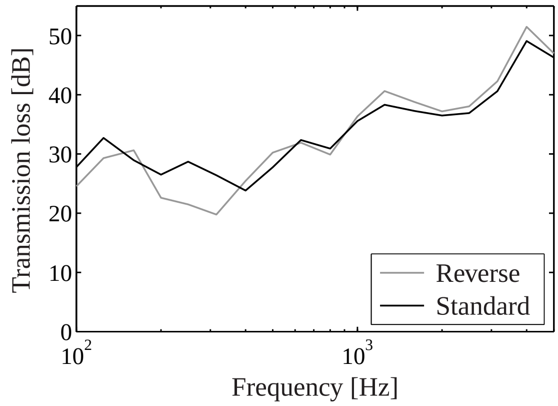

(b) Perforated HC sandwich panel

Fig. 11 Transmission loss of resonator panels with the resonator openings at the receiving side (standard) and with the resonator openings at the reverberation room side (reverse).

4 Validation

Fig. 12, Fig. 13 and Fig. 14 show the calculated and measured transmission loss of the three resonator panels in the frequency ranges of 500-3000 Hz and 500-5000 Hz, respectively. To enable a better comparison, the calculated transmission loss is corrected with the same frequency dependent factor as the mass law shown in equation

(17). The results are presented in narrow bands to show more detail. For all panels, the measured transmission loss is much smaller than predicted by the one-dimensional analytical model.

An explanation for the difference observed for panel with plastic tubes is that the ends of the tubes start to resonate in frequency range for which the resonators were tuned. This causes a difference in amplitude and phase between the ends of the tube and the part of the plate, which was not included in the model. To compensate for this effect, the model is corrected by including the measured amplitude difference and phase difference (in the frequency range of 500-2500 Hz). This lowers the transmission loss curve (see Fig. 12) and gives a possible explanation for the fact that the panel performs worse than the mass law in the higher frequency range. However, the agreement is still bad and the frequency of the maximum increase in transmission loss was measured much lower than predicted analytically. Possible resonances of the thin walls of the tubes might be a reason for these large discrepancies. This is currently under investigation.

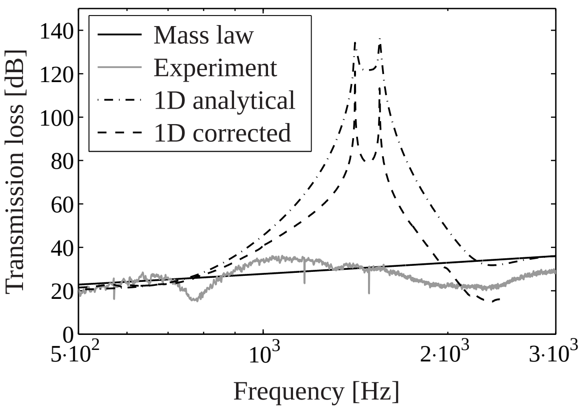

Fig. 12 Calculated and measured transmission loss of panel with plastic tubes.

For the panel with aluminium tubes, the centre frequency of the range in which the transmitted sound is reduced is predicted fairly well (see Fig. 13). However, the extra increase in transmission loss in the frequency range of 500-1200 Hz was not predicted analytically. This increase is even higher than measured in the frequency range for which the resonators were tuned.

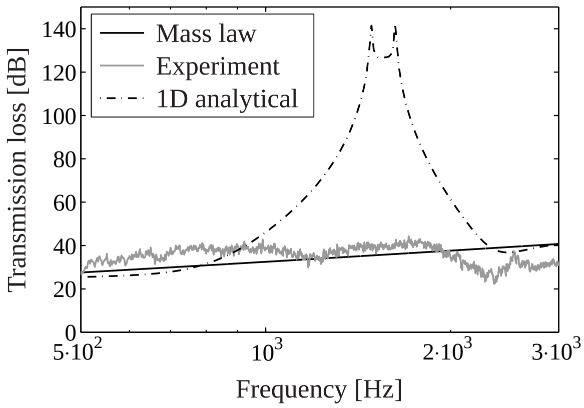

Fig. 13 Calculated and measured transmission loss of panel with aluminium tubes.

The trends of the measured and calculated transmission loss curves of the perforated HC sandwich panel are fairly similar (see Fig. 14). Around 1541 Hz, where half of the wavelength corresponds with the thickness of the panel, both transmission loss curves show a small dip caused by internal resonances in the cavities of the HC structure. Also the higher harmonic in the frequency range of 3000-5000 Hz is observed in both results. However, the frequency belonging to the peak of the measured transmission loss curve is a little lower than predicted analytically. Also for this panel an extra increase in transmission loss is observed in the lower frequency range, which is not predicted analytically.

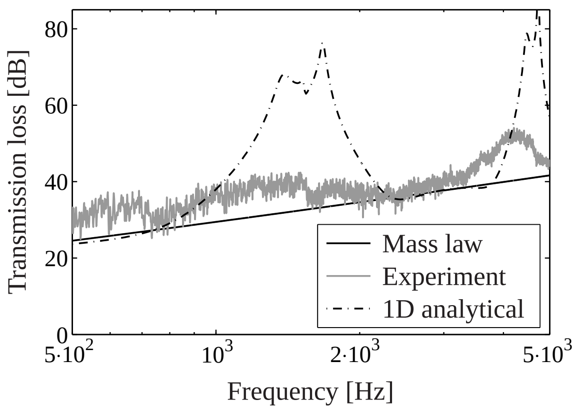

Fig. 14 Calculated and measured transmission loss of perforated HC sandwich panel.

5 Conclusions and discussion

Sound transmission loss measurements demonstrated that by applying tube resonators, the sound transmission loss of panels can be improved compared with the mass law. This was shown for two different configurations: panels with tubes and sandwich panels. A maximum increase in transmission loss of 9.2 dB was obtained for the perforated HC sandwich panel and of 7.1 dB for the panel with tubes. In the entire frequency range above the 500 Hz 1/3OB, the transmission loss of the perforated HC sandwich panel was larger than the mass law. However, for all panels, the increases were not as large as predicted by the one-dimensional analytical models presented in this paper. Moreover, the tube panels showed large decreases in transmission loss in the higher frequency ranges. The predictions for the perforated HC sandwich panels were a little better.

To give a better prediction of the transmission loss that can be obtained by panels with acoustic resonators, more detailed models are required. Possible causes for the discrepancies between the measurements and the results obtained with the one-dimensional models are the negative effects of: the flexibility of the panel, the flexibility of the resonators, acoustic coupling between the resonators, random incident sound, coincidence, and boundedness of the panel. Further research is needed and ongoing to study these effects [1].

Acknowledgements

This research has been performed in the framework of the EU-FP5 project FACE, contract number G4RD-CT2002-00764. The support of FACE is gratefully acknowledged. The experiments have been performed at the National Aerospace Laboratory NLR. Special thanks go to Henk van der Wal, Marko Beenders, Onno Stallinga and Corné Boons for this. Futhermore, the author would like to thank Ysbrand Wijnant, Ruud Spiering and André de Boer for their valuable suggestions and comments.

References

[1] M.H.C. Hannink, R.M.E.J. Spiering, Y.H. Wijnant, and A. de Boer. A finite element approach to the prediction of sound transmission through panels with acoustic resonators. In *Proceedings of ICSV13*, Vienna, Austria, 2006.

[2] M.H.C. Hannink and H. van der Wal. Design and testing of a 1 m × 1 m optimised trim panel. Technical Report FACE/TWE/5.1/TR-0003, Univeristy of Twente, The Netherlands, 2005.

[3] M.H.C. Hannink, J.P. Vlasma, Y.H. Wijnant, and A. de Boer. Application of acoustically tuned resonators for the improvement of sound insulation in aircraft. In *Proceedings of Internoise*, Rio de Janeiro, Brazil, 2005.

[4] F.P. Mechel. *Schallabsorber*. S. Hirzel Verlag, Stuttgart, 1995.

[5] J.H. Rindel. Sound transmission through single layer walls. In *Proceedings of Noise-93*, St. Petersburg, Russia, 1993.

[6] B.W. Ross and R.A. Burdisso. Low frequency passive noise control of a piston structure with a weak radiating cell. *Journal of the Acoustical Society of America*, 106(1):226–232, 1999.

[7] R.L. St. Pierre Jr., G.H. Koopmann, and W. Chen. Volume velocity control of sound transmission through composite panels. *Journal of Sound and Vibration*, 210(4):441–460, 1998.

[8] H. van der Wal and E. Geurts. Transmission loss measurements and modal testing on 2 m × 1.6 m curved panels; test set-up and experimental results. Technical Report FACE/NLR/6.1/TR-0016, National Aerospace Laboratory NLR, The Netherlands, 2004.